



# Facile synthesis of monodispersed Pd nanocatalysts decorated on graphene oxide for reduction of nitroaromatics in aqueous solution

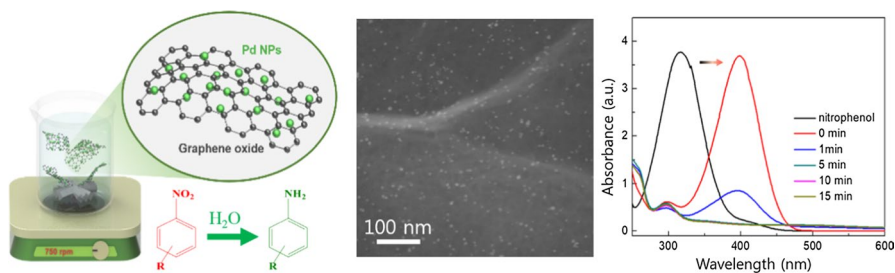
Kaiqiang Zhang, et al. [full author details at the end of the article]

Received: 15 August 2018 / Accepted: 28 September 2018 / Published online: 4 October 2018  
© Springer Nature B.V. 2018

## Abstract

We synthesized the reproducible heterogeneous catalyst of graphene oxide (GO)-supported palladium nanoparticles (NPs) via a simple and green process. The structure, morphology and physicochemical properties of the synthesized heterogeneous catalyst were characterized by the latest techniques such as high-resolution transmission electron microscopy (TEM), scanning TEM, energy-dispersive X-ray spectroscopy, X-ray diffraction analysis, and X-ray photoelectron spectroscopy. The GO-supported Pd NPs (Pd/GO nanocatalyst) exhibited excellent catalytic activity for the reduction of nitroaromatics to aminoaromatics in aqueous sodium borohydride. The nitroaromatics were converted to corresponding aminoaromatics with high yields (up to 99%) using Pd/GO nanocatalyst in aqueous solution. The hybrid heterogeneous catalyst showed 83% of conversion after six cycles in the reduction of nitrobenzene to aminobenzene. These features ensured the high catalytic activity of the introduced graphene oxide supported Pd nanocatalysts.

## Graphical abstract



**Keywords** Graphene oxide · Nanocatalyst · Nitroaromatic · Palladium · Reduction

## Introduction

Aromatic amines as essential raw materials for the production of pharmaceuticals, textile dyes, pigments, plastics, and pesticides play a significant role in chemical related industries [1–4]. Hydrogenation of the relatively toxic nitroaromatics to the eco-friendly aminoaromatics is a promising green approach producing high product yields with convenient operability. The current practical methods generally require hydrogen gas pressure and high temperature, which highly increase the cost of aminoaromatics production [5–7]. In addition, these processes are achieved predominantly by using toxic reductants, e.g. hydrazine, and organic solvents, which are not environmentally compatible [8]. Nowadays, researchers are focusing on the exploration of nanocatalysts with high catalytic activity, good sustainability, and environmentally friendly characteristics [9–11]. Thus, diverse nanocatalysts have been synthesized using a series of transition metals such as Pt, Ru, and Rh, by wet chemical and high temperature synthesis [12–15]. However, the development of effective, nontoxic, and handle-convenient procedure to produce active nanocatalysts for this transformation is still highly desirable [16].

Considering the eco-friendly concept, the exploration for the reduction of nitroaromatics in a green approach with a high efficiency is still arduous [17]. Although several innovative methods have been introduced to circumvent these issues, the environmental-friendly conversion of nitroaromatics to aminoaromatics is still very challenging [18]. The use of catalysts is very necessary for this conversion process, which can be simply classified as metal particle catalysts [19], bimetal catalysts [20], solid-supported catalysts [21], and magnetic supported catalysts [22]. However, many of these catalysts are prepared via complicated approaches hampering their proficiency and practicability [23].

Atomic layer graphene simply fabricated by using Scotch tape in 2004 [24] has been highlighted due to good thermal conductance ( $5000 \text{ W mK}^{-1}$ ), stable benzene ring structures, outstanding mobility of charge carrier ( $200,000 \text{ cm}^2 \text{ Vs}^{-1}$ ), exhibition of high theoretical specific surface area ( $2600 \text{ m}^2 \text{ g}^{-1}$ ), and feasible large-scale production [25]. Graphene is a desirable support material for stabilizing catalytic nanoparticles (NPs) such as Au, Pd, and Pt to synthesis supported nanocatalysts with high activity, durability, and reusability. Such heterogeneous catalysts have been applied for variable organic transformations [26–28]. However, synthesis of uniform and well-dispersed Pd NPs on graphene oxide (Pd/GO) for the reduction of nitroaromatics to aminoaromatics by green and simple technique has been confined.

To pursue a facile method for the synthesis of supported nanocatalysts, we prepared the heterogeneous Pd/GO nanocatalyst by the stabilizing the Pd NPs on the surface of GO using Pluronic F127, which is a mild reductant and surfactant, and a water soluble copolymer. Then, we verified the prepared catalyst efficiency on catalytic activity, recyclability, and selectivity by reducing the nitroaromatics to aminoaromatics with aqueous sodium borohydride ( $\text{NaBH}_4$ ) solution. The nitroaromatics were totally converted to aminoaromatics in 10 min using a very small amount of Pd NPs. The hybrid heterogeneous nanocatalyst showed 83% of

conversion rate after six cycles reuse in the reduction of nitrobenzene to aminobenzene. Furthermore, various nitroaromatics possessing different functional groups were selectively reduced into their corresponding aminoaromatics in 10 min, exclusively.

## Experimental

### Materials and characterizations

Water was deionized by a Nano Pure System (Barnsted). The organic reagents and F127 used in this work were purchased at the highest possible grade from Samchun Co., Ltd. and Daejung Co., Ltd. Potassium tetrachloropalladate ( $K_2PdCl_4$ ) and  $NaBH_4$  were purchased from SigmaAldrich. X-ray photoelectron spectroscopy (XPS) was performed using an Al  $K\alpha$  source (Sigma probe, VG Scientifics). The nanostructure of the prepared Pd/GO was studied using a high resolution X-ray diffraction (XRD, D8-Advance), a transmission electron microscope (TEM, JEOL JEM-3010) equipped with an energy-dispersive X-ray spectroscopy (EDX) detector, a scanning TEM (STEM, JEOL JEM-2100F), a thermal gravimetric analysis (TGA, simultaneous DTA/TGA analyzer), and an infrared radiation (IR, Nicolet iS50). The loading amount of Pd NPs on the graphene was measured through an inductively coupled plasma atomic emission spectroscopy (ICP-AES, ICPS-8100). The ICP samples were prepared by dissolving the dried Pd/GO samples in a 4 mL of *aqua regia* solution. Ultraviolet-visible (UV-Vis) absorption spectra (V-770 JASCO) and gas chromatography-mass spectrometry (GC-MS, Agilent 7890A Gas chromatograph and 5977A Mass selective detector) were employed to monitor the reduction processes and the conversion rate of the nitroaromatics to aminoaromatics, respectively.

### Preparation of graphene oxide

Graphene oxide was synthesized from graphite using the modified Hummer's approach [29]. In a typical synthesis, commercial graphite powder (10 g) was added into 230 mL concentrated  $H_2SO_4$  that had been cooled to below 20 °C with a circulator, and 300 g potassium permanganate was added while stirring. Then, the temperature of the reaction was adjusted to 40 °C and the mixture was stirred for 1 h. Water (500 mL) was added to the mixture and the temperature was increased to 100 °C. After that, 2.5 mL  $H_2O_2$  (30 wt%) was slowly added to the mixture. For purification, the suspension was washed with HCl solution (200 mL) using a filter and a funnel. The suspension was washed with water several times until the filtrate became neutral.

### Preparation of Pd/GO nanocatalyst

Pd/GO nanocatalyst was simply synthesized via a mixing process at room temperature. In a typical synthesis, 30 mL of GO solution ( $5 \text{ mg mL}^{-1}$ ) was added in a beaker and stirred at room temperature, followed by the introduction of Pluronic

F-127 aqueous solution (2 g). Finally,  $K_2PdCl_4$  (100 mg) was added into the solution and stirred for 10 h at room temperature to produce Pd NPs supported on the GO. The suspension was filtered and thoroughly washed with hot water and ethanol. The prepared heterogeneous catalyst was finally redispersed in water. The total concentration of the prepared Pd/GO solution was  $30\text{ mg mL}^{-1}$ .

### Catalytic reduction of nitroaromatics

The reduction of nitrophenol to aminophenol with  $NaBH_4$  was catalyzed using Pd/GO nanostructured catalyst at room temperature. This reaction was thoroughly achieved within 10 min. The hydrogenation process from nitrophenol to aminophenol was monitored by measuring the UV–Vis absorption spectra of the reactants and products. Similarly, the reduction of other nitroaromatics was performed in water at room temperature. In a typical procedure, the Pd/GO nanocatalyst ( $20\ \mu\text{L}$ ) was dispersed in 15 mL  $H_2O$ . Then, a nitroaromatic (1 mmol),  $NaBH_4$  (1.2 mmol) and a small stirring bar were added into a glass flask. The reaction mixture was stirred at room temperature for 10 min under air atmosphere. After completion of reaction, the Pd/GO nanostructured catalyst was separated using a centrifuge. The yields of the reduced products were determined by GC–MS.

### Results and discussion

The overall synthetic procedure is illustrated in Fig. 1. Pd NPs were simply inlaid on the surface of the GO sheets to produce highly catalytic active heterogeneous Pd/GO nanostructured catalyst. The morphology of the GO and Pd/GO nanocatalyst were displayed by STEM (Fig. 2a, b). The small Pd NPs ( $\sim 5\text{ nm}$ ) could be decorated on the surface of GO uniformly and discretely, which enhance their exposed active sites and specific surface area of Pd/GO nanocatalyst. The EDX mapping results (Fig. 2c–e) further demonstrated the well-distribution of Pd NPs on the GO and we successfully made the reproducible Pd/GO nanostructured catalyst by a green and simple approach. TEM images (Fig. 3b, c) also confirmed a similar result of uniform Pd NPs decorated on GO. The density of Pd

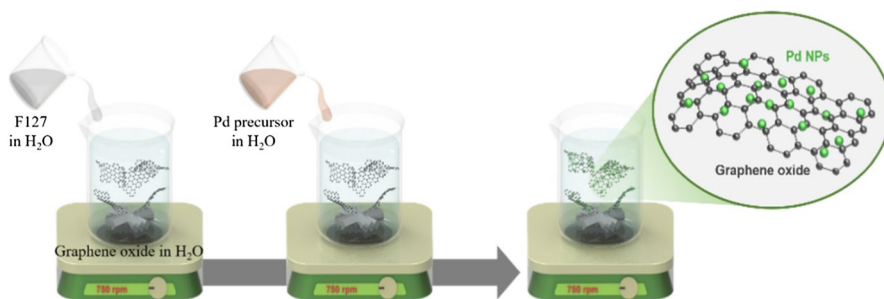


**Fig. 1** Procedure for the synthesis of Pd/GO nanocatalyst

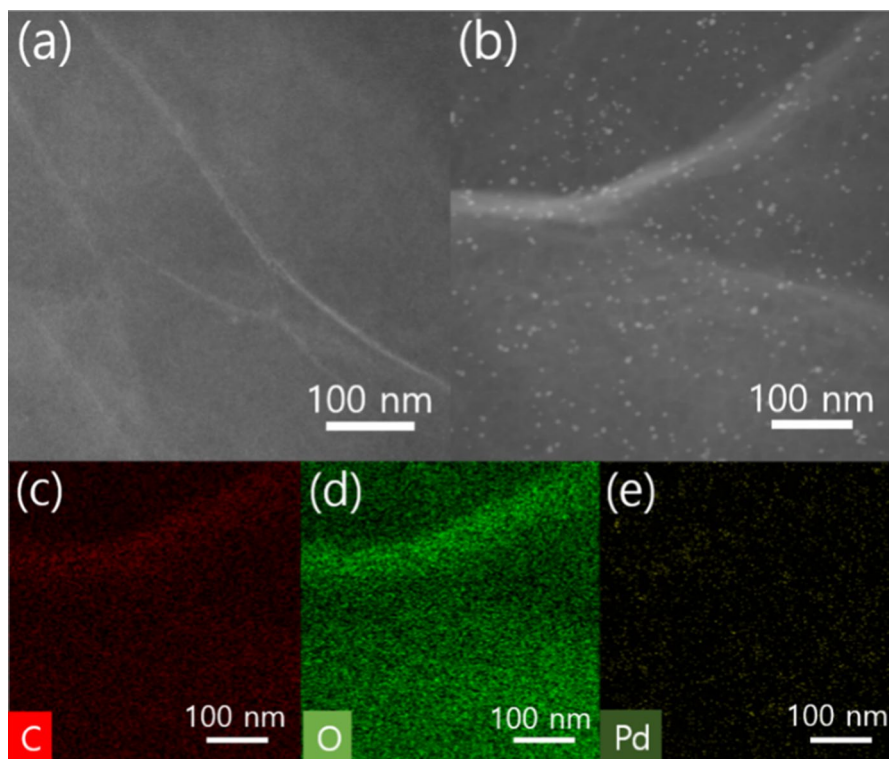


**Fig. 2** STEM micrographs of **a** GO and **b** Pd/GO nanocatalyst. EDX mapping images of **c** C, **d** O, and **e** Pd

NPs distribution is about  $510 \mu\text{m}^{-1}$ . The presence of Pd NPs on GO support does not show any detachable damage and we can clearly see the existence of ripples in GO sheets. In addition, the HRTEM image (Fig. 3d) shows fine crystalline Pd NPs with  $\sim 5$  nm of diameter. The small-size Pd NPs on the GO surface significantly contribute to widening the specific surface area to enhance the contact with nitroaromatics in the reduction process. TEM images also shows similar results so that Pd NPs uniformly are loaded on the GO. The EDX spectrum distinctly confirms the existence of carbon and Pd species in Pd/GO.

We employed XRD characterizations in order to further study the crystal structure of both GO and Pd/GO catalyst. The XRD result of GO shows a peak at  $10.90^\circ$  indicating a disorder stack of the GO layers (Fig. 4). However, the appearance of major peaks at  $2\theta = 40.02^\circ$ ,  $46.59^\circ$ ,  $68.08^\circ$ ,  $82.90^\circ$  in XRD patterns of the Pd/GO corresponding to (111), (200), (220), (311) (JCPDS 01-087-0641) clearly demonstrates the successful decoration of Pd NPs loading on GO. The surface stabilities of the GO and Pd/GO were confirmed by the FT-IR (Fig. 5). A strong absorption band at  $3450 \text{ cm}^{-1}$  (O–H stretching vibrations) in the case of GO indicates a heavy residual of  $\text{H}_2\text{O}$  than Pd/GO even after sufficient drying.

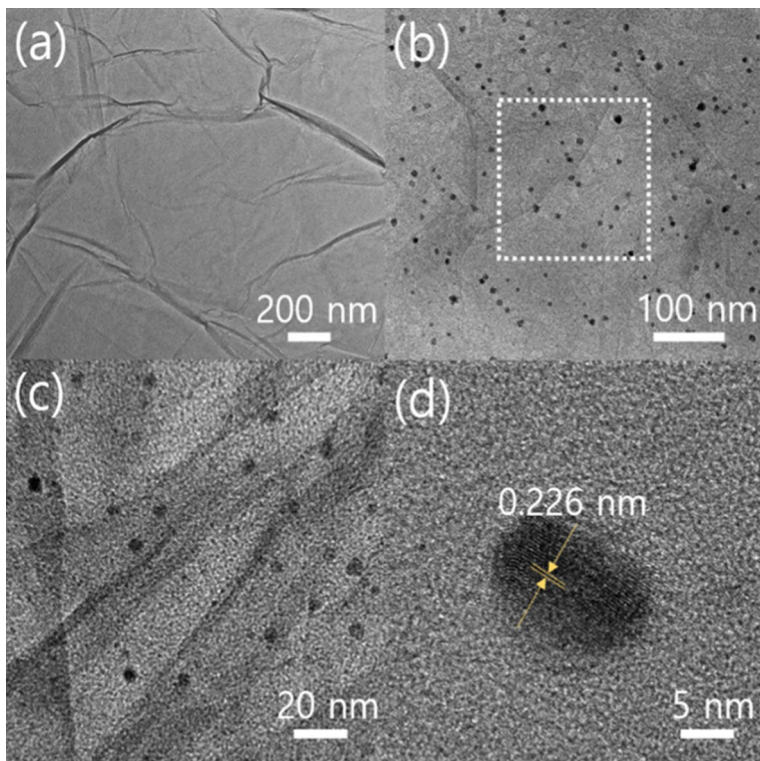


**Fig. 3** TEM images of **a** GO, and **b** and **c** Pd/GO nanocatalyst. **d** HRTEM image of Pd/GO nanocatalyst

**Fig. 4** XRD patterns of GO and Pd/GO nanocatalyst

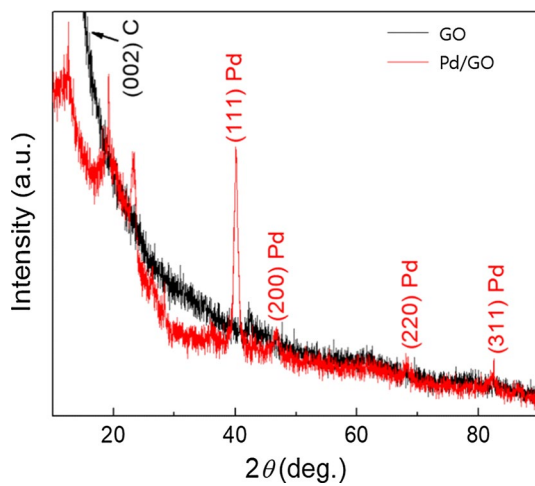
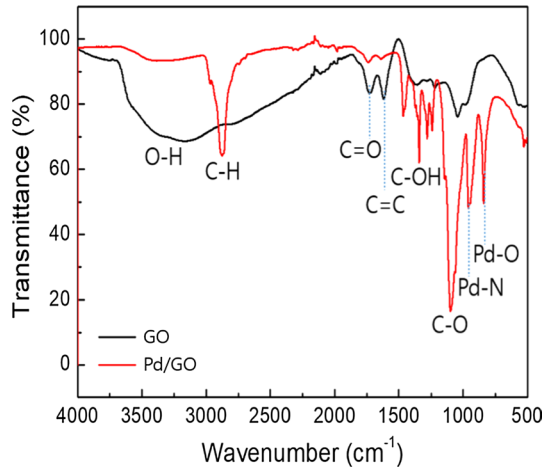
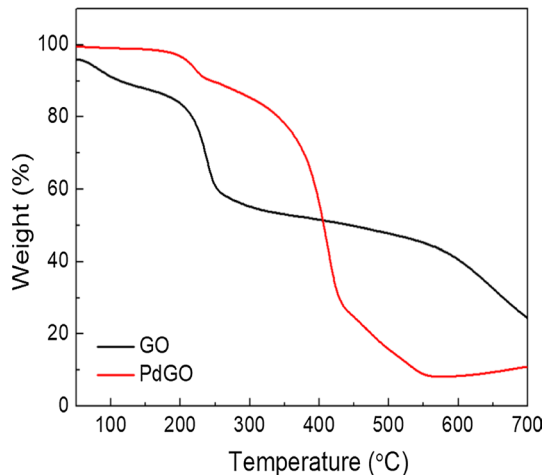


**Fig. 5** FT-IR spectra of GO and Pd/GO nanocatalyst



In addition, the characteristic absorption bands are at  $1725\text{ cm}^{-1}$  for the C=O stretching vibrations,  $1600\text{ cm}^{-1}$  for the C=C (skeletal vibrations of graphene) in GO. However, those two peaks decreased in Pd/GO denoting the reduction of F127. The differences in FT-IR demonstrate the changes in the structures after Pd loading, which is also captured in the TGA analysis for both GO and Pd/GO (Fig. 6). The weight loss ( $\sim 16\%$ ) in the GO is due to the loss of intercalated water molecules, followed by the second rapid drop corresponding to the decomposition of functional groups at around  $200\text{ }^{\circ}\text{C}$ , whereas the weight loss of  $\sim 5\%$  for Pd/GO suggests the presence of a little moisture in the prepared nanostructured catalyst. This demonstrates that the moisture and labile oxygen functional groups were removed after the introduction of the mild F127. An abrupt increase in the weight loss at  $\sim 400\text{ }^{\circ}\text{C}$  for the Pd/GO can be ascribed by the remove of F127. We

**Fig. 6** TGA results of GO and Pd/GO nanocatalyst



assumed the mechanism of the loading Pd NPs on the GO is due to the reduction effect of F127 with OH functional groups, which is the reducing agent for the Pd ions. After this process, the OH functional groups were transferred into carbonyl groups.

The XPS analysis for the Pd/GO nanocatalyst is shown in Fig. 7. The XPS spectrum demonstrates the surface composition of the Pd/GO nanocatalyst, and the existence of Pd NPs on the GO. This also indicates a significant reduction of the oxygen functional groups as a consequence of the reduction process with Pluronic F127. The Pd ions in the solution interacted with the oxygen functional groups of the GO due to the electrophilic property of Pd generating Pd–O linkage, which facilitate the anchoring of Pd on the surface of GO. In addition, the existing functional defect sites on the GO can reduce the mobility of Pd ions, which further avoids the aggregation and facilitate the retaining of Pd NPs.

The catalytic reduction of the nitrophenol with  $\text{NaBH}_4$  by Pd/GO was chosen as a model reaction for the evaluation of catalytic activity. Figure 8 shows the UV–Vis absorption spectra emerging the change in concentration of the nitrophenol. The original adsorption peak of nitrophenol at 317 nm red shifted to 400 nm after the

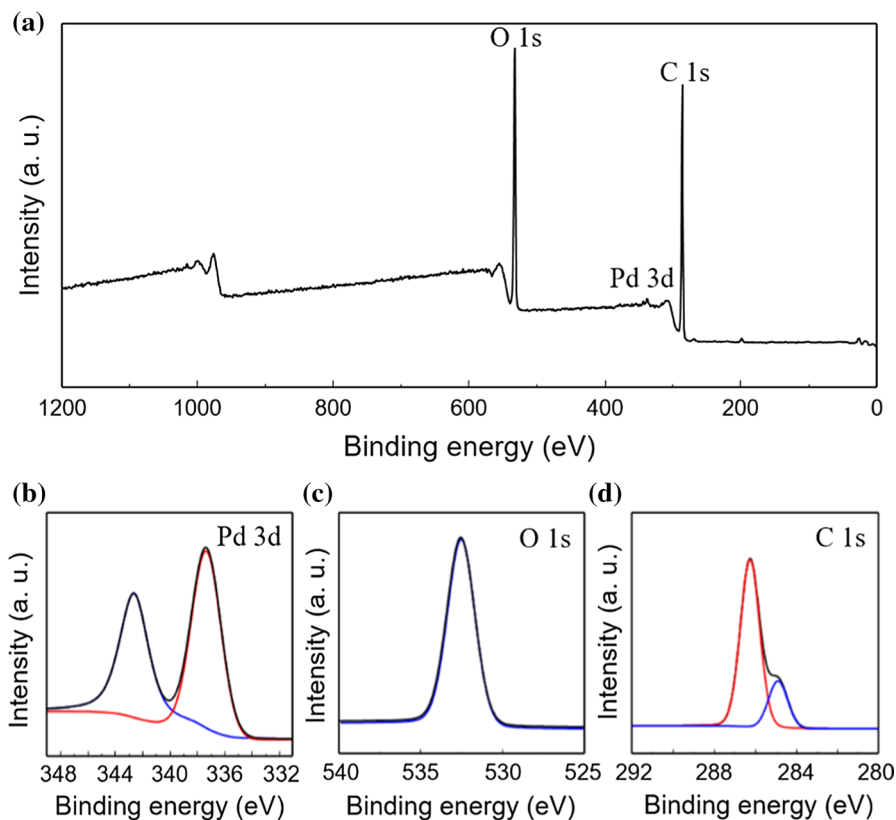
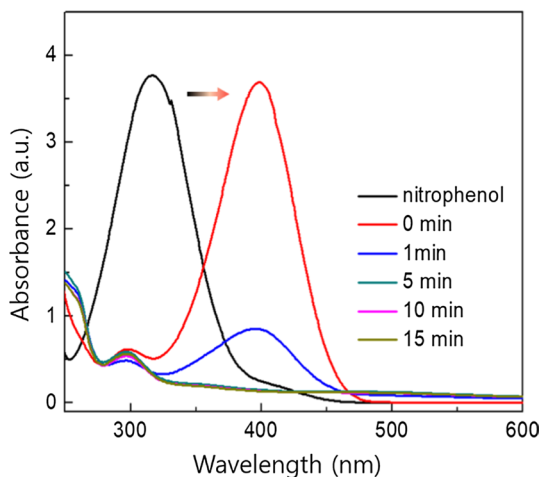


**Fig. 7** XPS analysis of **a** survey scan, and **b** Pd 3d, **c** C 1s, and **d** O 1s for the Pd/GO nanocatalyst



**Fig. 8** UV–Visible spectra of the catalytic reduction using Pd/GO nanocatalysts. Nitrophenol (1 mmol) was reduced in the presence of  $\text{NaBH}_4$  (1.2 mmol) by Pd/GO nanocatalyst (20  $\mu\text{L}$ ) in water



addition of  $\text{NaBH}_4$  solution accompanied with the color change from green yellow to bright yellow (Fig. 8, insets), which is due to the formation of nitrophenolate ions.  $\text{NaBH}_4$  appears alkaline in aqueous, therefore, the  $\text{H}^+$  from the hydroxyl of nitrophenol will be captured within a short time, causing the formation of nitrophenolate [30–33]. After the injection of Pd/GO, the peak intensities at 400 nm suddenly decreased due to the conversion and an absorption peak of aminophenol shown at 300 nm [34]. The complete reduction of nitrophenol to aminophenol took  $\sim 10$  min. This process was fulfilled very fast considering the use of a very small amount of Pd NPs in water. This excellent catalytic activity can be explained by two main reasons. First, the nano-sized Pd particles anchored on graphene without obvious aggregation enabled active sites sufficiently exposed in ambient air, which provided enough electron transfer channels during hydrogenation. Second, the employment of the nanocatalysts in the reduction processes reduced the barrier energy, and a decreased barrier energy was provided by small-sized Pd nanocatalysts, which affords a rapid electron transfer rate [35–39]. The reduction process of nitrophenol with  $\text{NaBH}_4$  in this study can be explained according to the previously proposed mechanism [40, 41].

We also investigated the reductive activity of Pd/GO nanocatalyst for the nitroaromatics with various substituents as shown in Table 1. Pd/GO nanocatalyst presented a high catalytic activity for the reduction of diverse functionalized nitroaromatic compounds in 10 min. The high hydrogenation activity of the Pd/GO nanocatalyst can be ascribed to the  $\pi$  bond between the nitroaromatics and graphene oxide and the reactants accumulation on the surface of the supported Pd NPs, promoting the contact of reactants and the nanocatalysts [42].

When we compared the catalytic activity of the Pd/GO nanocatalyst with the previously published nanocatalysts in the reduction of nitrophenol, a very competitive yield of aminophenol was obtained (Table 2). The Pd/GO nanocatalyst also presented higher catalytic activity than the commercially available Pd/C catalyst. The

**Table 1** Heterogeneous reduction of nitroaromatics by Pd/GO nanocatalyst

| Entry | Substrate | Product | Yield (%) |
|-------|-----------|---------|-----------|
| 1     |           |         | 99        |
| 2     |           |         | 99        |
| 3     |           |         | 97        |
| 4     |           |         | 94        |
| 5     |           |         | 99        |
| 6     |           |         | 85        |
| 7     |           |         | 83        |

Reaction conditions: substituted nitroarenes (1 mmol), NaBH<sub>4</sub> (1.2 mmol), Pd/GO nanocatalyst (20 μL), H<sub>2</sub>O (15 mL), room temperature, 10 min. The yields were determined by GC-MS

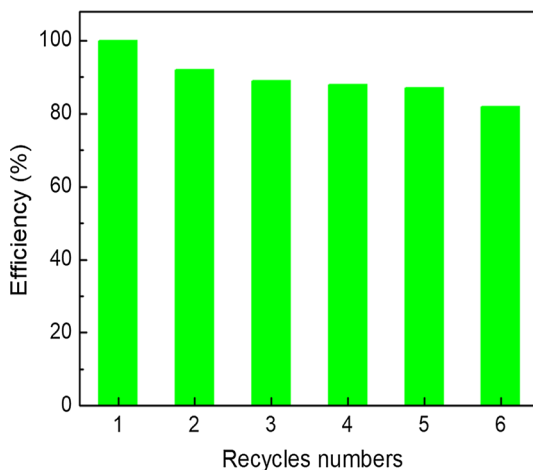
**Table 2** Catalytic comparison studies of known heterogeneous catalysts in the reduction of nitrophenol using  $\text{NaBH}_4$ 

| Entry | Catalyst                             | Amount (mg) | Time(min) | References |
|-------|--------------------------------------|-------------|-----------|------------|
| 1     | Ni@Pd/KCC-1                          | 0.4         | 5         | [44]       |
| 2     | Pd@black tea                         | 2           | 1.3       | [45]       |
| 3     | Pd loaded $\text{TiO}_2$ nanotube    | 1           | 7         | [46]       |
| 4     | Aluminium hydroxide supported Pd NPs | 25          | 6         | [47]       |
| 5     | $\text{CeO}_2/\text{Pd}$             | 10          | 1         | [48]       |
| 6     | Pd/GO                                | 5           | 10        | This work  |

commercial catalyst provided a much lower yield (39%) when it was used in the reduction of nitrobenzene with  $\text{NaBH}_4$  under the identical reaction conditions.

Recycling and reusing the precious nanocatalysts are very important criteria for their practical applications [43]. The reusability of the Pd/GO nanocatalyst was conducted for the reduction of nitrobenzene. We repeated the same reduction process for six runs. The Pd/GO nanocatalyst were collected using a centrifuge and washed with deionized water several times. Subsequently, the Pd/GO nanocatalyst was dried in an oven and applied for the next catalytic processes. The yields showed a gradually decrease in conversion rate so that 83% of conversion ratio was observed after six runs (Fig. 9). The centrifugation assisted to achieve an almost thoroughly separation of Pd/GO nanocatalyst from the aqueous, by which resulting in the loss of Pd/

**Fig. 9** The conversion of nitrobenzene to aminobenzene. Nitrobenzene (1 mmol) was reduced in the presence of  $\text{NaBH}_4$  (1.2 mmol) by Pd/GO nanocatalyst (20  $\mu\text{L}$ ) in 10 min



GO nanocatalyst due to the adhesion on the centrifuge tube. This inevitable loss reduced the conversion of nitroaromatics to aminoaromatics.

## Conclusions

In this study, we prepared the graphene oxide supported Pd nanoparticles (Pd/GO nanocatalyst) by employing the cost-efficient pluronic F127 via a simple and green one-step preparation. A remarkable high catalytic activity was shown for the selective reduction of nitroaromatics to aminoaromatics. Of particular note of this procedure is that the Pd/GO nanocatalyst could be reused for six consecutive cycles in the reduction of nitrobenzene. The excellent catalytic activity of Pd/GO nanocatalyst for the nitroaromatic reductions can be ascribed to the uniform dispersion and high surface area/volume ratio of Pd nanoparticles on GO. This work provided a modifying concept for hydrogenation of nitroaromatics that may stimulate further exploration of nanocatalysts with low-cost and high-efficiency for nitroaromatics reduction.

**Acknowledgements** This research was financially supported by the New and Renewable Energy Core Technology Program of the Korea Institute of Energy Technology Evaluation and Planning (KETEP) funded by the Ministry of Trade, Industry & Energy, Republic of Korea (No. 20143030031430). This work also supported in part by the Energy Efficiency and Resources Core Technology Program of the KETEP granted financial resource from the Ministry of Trade, Industry and Energy, Republic of Korea (No. 20152020106100).

## Compliance with ethical standards

**Conflicts of interest** The Authors declare that they have no conflict of interest.

## References

1. H.U. Blaser, C. Malan, B. Pugin, F. Spindler, H. Steiner, M. Studer, *Adv. Synth. Catal.* **345**, 103 (2003)
2. O. Verho, K.P.J. Gustafsson, A. Nagendiran, C.W. Tai, *ChemCatChem* **6**, 3153 (2014)
3. R.J. Rahaim, R.E. Maleczka, *Org. Lett.* **7**, 5087 (2005)
4. F.A. Westerhaus, R.V. Jagadeesh, G. Wienhofer, M.M. Pohl, J. Radnik, A.E. Surkus, J. Rabeah, K. Junge, H. Junge, M. Nielsen, *Nat. Chem.* **5**, 527 (2013)
5. M. Shokouhimehr, T. Kim, S.W. Jun, K. Shin, Y. Jang, B.H. Kim, J. Kim, T. Hyeon, *Appl. Catal. A* **476**, 133 (2014)
6. M. Shokouhimehr, J.E. Lee, S.I. Han, T. Hyeon, *Chem. Commun.* **49**, 4779 (2013)
7. Z. Dong, X. Le, Y. Liu, C. Dong, J. Ma, J. Mater. Chem. A **2**, 18775 (2014)
8. Z. Dong, X. Le, X. Li, W. Zhang, C. Dong, J. Ma, *Appl. Catal. B-Environ.* **158**, 129 (2014)
9. F. Zaera, *Chem. Soc. Rev.* **42**, 2746 (2013)
10. M. Shokouhimehr, *Catalysts* **5**, 534 (2015)
11. A. Kim, S. Abdolhosseini, S.M. Rafiaei, M. Shokouhimehr, *Energy Environ. Focus* **4**, 18 (2015)
12. X. Cui, Y. Long, X. Zhou, G. Yu, J. Yang, M. Yuan, J. Ma, Z. Dong, *Green Chem.* **20**, 1121 (2018)
13. S. Sharma, D. Bhattacharjee, P. Das, *Adv. Synth. Catal.* **360**, 2131 (2018)
14. E. Yilmaz, M. Soylak, *J. Iran. Chem. Soc.* **14**, 2503 (2017)
15. P. Zhang, X. Yang, H. Peng, D. Liu, L. Lu, J. Wei, J. Gui, *Catal. Commun.* **100**, 214 (2017)
16. E. Yilmaz, Y. Tut, O. Turkoglu, M. Soylak, *J. Iran. Chem. Soc.* **15**, 1721 (2018)
17. A.M. Tafesh, J. Weiguny, *Chem. Rev.* **96**, 2035 (1996)

18. H. Wu, L. Zhuo, Q. He, X. Liao, B. Shi, *Appl. Catal. A* **366**, 44 (2009)
19. K.J. Datta, A.K. Rath, P. Kumar, J. Kaslik, I. Medrik, V. Ranc, R.S. Varma, R. Zboril, M.B. Gawande, *Sci Rep.* **7**, 11585 (2017)
20. H. Li, Z. Zhu, J. Liu, S. Xie, H. Li, *J. Mater. Chem.* **20**, 4366 (2010)
21. M. Shokouhimehr, J.H. Kim, Y.S. Lee, *Synlett* **4**, 618 (2006)
22. M. Shokouhimehr, K.Y. Shin, J.S. Lee, M.J. Hackett, S.W. Jun, M.H. Oh, J. Jang, T. Hyeon, *J. Mater. Chem. A* **2**, 7593 (2014)
23. M.B. Gawande, P. Branco, R.S. Varma, *Chem. Soc. Rev.* **42**, 3371 (2013)
24. M.J. Allen, V.C. Tung, R.B. Kaner, *Chem. Rev.* **110**, 132 (2009)
25. A.K. Geim, *Science* **324**, 1530 (2009)
26. S. Moussa, A.R. Siamaki, B.F. Gupton, M.S. El-Shall, *ACS Catal.* **2**, 145 (2012)
27. A.R. Siamaki, A.E.R.S. Khder, V. Abdelsayed, M.S.E. Shall, B.F. Gupton, *J. Catal.* **279**, 1 (2011)
28. M. Gomez-Martinez, E. Buxaderas, I.M. Pastor, D.A. Alonso, *J. Mol. Catal. A Chem.* **404**, 1 (2015)
29. W.S. Hummers, R.E. Offeman, *J. Am. Chem. Soc.* **80**, 1339 (1958)
30. M.M.D. Anna, S. Intini, G. Romanazzi, A. Rizzuti, C. Leonelli, F. Piccinni, P. Mastrorilli, *J. Mol. Catal. A: Chem.* **395**, 307 (2014)
31. A. Krogul-Sobczak, P. Kasperska, G. Litwinienko, *Catal. Commun.* **104**, 86 (2018)
32. S.S. Kotha, N. Sharma, G. Sekar, *Tetrahedron Lett.* **57**, 1410 (2016)
33. Q. Hu, X. Liu, L. Tang, D. Min, T. Shi, W. Zhang, *RSC Adv.* **7**, 7964 (2017)
34. M.M. Ayad, W.A. Amer, M.G. Kotp, *Mol. Catal.* **439**, 72 (2017)
35. W. Wang, Y. Xi, S. Zhang, X. Liu, M. Haruta, J. Huang, *Catalysts* **8**, 60 (2018)
36. E. Menumerov, R.A. Hughes, S. Neretina, *Nano Lett.* **16**, 7791 (2016)
37. Z. Wu, X. Yuan, H. Zhong, H. Wang, G. Zeng, X. Chen, H. Wang, L. Zhang, J. Shao, *Sci. Rep.* **6**, 25638 (2016)
38. M. Shokouhimehr, M.S. Asl, B. Mazinani, *Res. Chem. Intermed.* **44**, 1617 (2018)
39. A. Haghighatzadeh, B. Mazinani, M. Shokouhimehr, L. Samiee, *Desalin. Water Treat.* **92**, 145 (2018)
40. Y. Du, H. Chen, R. Chen, N. Xu, *Appl. Catal. A Gen.* **277**, 259 (2004)
41. J. Huang, T. Jiang, H. Gao, B. Han, Z. Liu, W. Wu, Y. Chang, G. Zhao, *Angew. Chem. Int. Ed.* **43**, 1397 (2004)
42. R. Kuwano, M. Kashiwabara, *Org. Lett.* **8**, 2653 (2006)
43. M. Shokouhimehr, K. Hong, T.H. Lee, C.W. Moon, S.-P. Hong, K. Zhang, J.M. Suh, K.S. Choi, R.S. Varma, H.W. Jang, *Green Chem.* **20**, 3809 (2018)
44. Z. Dong, X. Le, C. Dong, W. Zhang, X. Li, J. Ma, *Appl. Catal. B Environ.* **162**, 372 (2015)
45. S. Lebaschi, M. Hekmati, H. Veisi, *J. Colloid Inter. Sci.* **485**, 223 (2017)
46. V. Kalarivalappil, C.M. Divya, W. Wunderlich, S.C. Pillai, S.J. Hinder, M. Nageri, V. Kumar, B.K. Vijayan, *Catal. Lett.* **146**, 474 (2016)
47. H. Goksu, *New J. Chem.* **39**, 8498 (2015)
48. R. Ma, Y. Kim, D.A. Reddy, T.K. Kim, *Ceram. Int.* **41**, 12432 (2015)

## Affiliations

Kaiqiang Zhang<sup>1</sup> · Kootak Hong<sup>1</sup> · Jun Min Suh<sup>1</sup> · Tae Hyung Lee<sup>1</sup> · Ohkyung Kwon<sup>2</sup> · Mohammadreza Shokouhimehr<sup>1</sup> · Ho Won Jang<sup>1</sup>

✉ Mohammadreza Shokouhimehr  
mrsh2@snu.ac.kr

✉ Ho Won Jang  
hwjang@snu.ac.kr

<sup>1</sup> Department of Materials Science and Engineering, Research Institute of Advanced Materials, Seoul National University, Seoul 08826, Republic of Korea

<sup>2</sup> National Instrumentation Center for Environmental Management, Seoul National University, Seoul 08826, Republic of Korea